RESEARCH ARTICLE

Key Points:
- We study MCs encountered STEREO A and B and ACE independently and in comparison
- Annual MC counts at each spacecraft vary and do not follow the solar activity
- Statistically, halo CMEs are poor predictors of MCs

Correspondence to:
Y. Li,
yanli@ssl.berkeley.edu

Magnetic clouds and origins in STEREO era

Yan Li[1], J. G. Luhmann[1], B. J. Lynch[1], and E. K. J. Kilpua[2]

[1]Space Sciences Laboratory, University of California, Berkeley, California, USA, [2]Department of Physics, Division of Atmospheric Sciences and Geophysics, University of Helsinki, Helsinki, Finland

Abstract When a coronal mass ejection (CME) encounters the Earth, the Earth's electromagnetic environment is disturbed, especially when it is a magnetic cloud (MC) with enhanced, steady, and long-lasting southward field. The speed and the magnetic field of an MC are the two important properties for its geoeffectiveness. The correspondence between a CME and its resulting MC is not straightforward, partly due to the CME velocity and the complications during propagation through corona and the solar wind. From 2007 to 2012, we have three observing points at 1 AU near the ecliptic plane (ACE and STEREO A and B). We search for MC events encountered at one of the three observers and study the statistics independently and in comparison. We found that the annual number of MCs at each receiver varies significantly and the temporal variation at each receiver does not always follow the solar activity level. The speed and the magnetic field strength of the MCs do vary with the solar activity level. The polarity of MC magnetic field at ACE and STEREO also shows large fluctuations. We have also identified the CME and solar activity sources for the L1 MC events. STEREO SECCHI images served critical roles in the determination of the CMEs both in solar quiet times and active times. We found that halo CMEs are not necessarily good indicators for receiving MCs. Further studies of CME initial velocity and the propagation through the heliosphere are needed in order to improve our space weather forecasting capability.

1. Introduction

Coronal mass ejection (CME) is a major space weather driver, especially when their interplanetary counterparts are in the form of magnetic clouds (MCs) and these encounter the Earth. MCs carry enhanced magnetic field and out-of-ecliptic plane magnetic field. CMEs also cause disturbance of the ambient solar wind and interplanetary magnetic field (IMF), and fast CMEs drive shocks and generate energetic particles. Since 2007, we have STEREO twin spacecraft orbiting the Sun about 1 AU near the ecliptic plane in addition to the ACE spacecraft, making three independent observing points of the in situ solar wind and IMF near the ecliptic plane and 1 AU during an extended period for the first time.

Several issues about CMEs need to be understood in order to improve our space weather forecasting capability. First, the initiation; second, what determines the speed and direction; third, what determines CME magnetic field magnitude, polarity and structure; and fourth, CME propagation in the corona and through the interplanetary space.

When a halo CME is seen in the coronagraph, it is usually taken as the sign that the CME is heading toward (frontside) or away (backside) from the Earth (observer). Whether a frontside halo CME will actually encounter the Earth is not clear. *Webb et al.* [2000] studied the relationship between halo CMEs, magnetic clouds (MCs), and geomagnetic storms. They analyzed 14 halo CMEs from the post solar minimum years 1996 and 1997 and found that seven are associated with solar disk activity. They further found that the location of the solar activity for six of the seven frontside halo CMEs was within $0.5R_\odot$ of the Sun center and had geoactivity 3 to 5 days later. By analysis of 36 Earth-directed halo CMEs, *Cane et al.* [2000] suggested that the locations of typical geoeffective solar events are within longitude 40° east and west. *Gopalswamy et al.* [2008] found that CMEs originating near the central meridian within average longitude about 17° will not miss the Earth. *Gopalswamy et al.* [2007] found that 71% halo CMEs during 1996 to 2005 are geoeffective using *Dst* index without identifying MCs.

Other studies found that CMEs can be deflected in the low corona by the magnetic structure, such that during solar minimum times, CMEs are mostly deflected toward lower latitudes than their source regions and during solar maximum time, the deflections of CMEs have no particular trend [*Cremades et al.*, 2006; *Kilpua et al.*, 2009]. It has also been found that CMEs undergo east-west deflections during the propagation in the

Table 1. L1 Magnetic Clouds and Origins in 2007–2012

MC		CME		Solar Disk Activity				
Time	V (km/s)	Halo	P.Halo	Flare	Other	Unclear	None	
2007-01-14 11:45	354	15.2	-	-	-	-	unclear	-
2007-05-21 22:45	456	14.8	-	05-19 13:24	B9.5 N03W07	FE[a]	-	-
2007-11-20 00:45	479	14.6	-	-	-	-	-	none
2008-03-08 17:45	390	16.5	-	-	-	FE S10W15	-	-
2008-09-03 16:30	433	13.5	-	08-30 17:30	-	-	-	none
2008-09-17 04:00	410	7.2	-	-	-	-	unclear	-
2008-12-17 03:30	403	9.5	-	12-12 08:54	-	FE N50W20	-	-
2009-02-04 00:00	380	11	-	-	-	-	-	none
2009-03-03 12:00	390	11	-	-	-	-	unclear	-
2009-03-12 18:00	380	17	-	-	-	-	-	none
2009-07-21 04:20	350	8	-	-	-	-	unclear	-
2009-08-05 12:00	380	12	-	-	-	-	unclear	-
2009-09-30 06:00	350	10	-	-	-	-	unclear	-
2009-10-22 12:00	350	10	-	10-17 20:58	-	dimming S30E15	-	-
2009-10-29 06:50	350	12	-	-	-	-	unclear	-
2010-04-05 12:00	700	10	04-03 10:33	-	B7.4 S23W17	dimming	-	-
2010-04-12 00:00	400	12	-	04-08 04:54	B3.7 N24W00	dimming	-	-
2010-05-18 12:00	300	9	-	-	-	-	unclear	-
2010-05-28 23::00	390	15	05-23 18:06	-	B1.1	FE N20E10	-	-
2010-06-21 11:00	290	7	-	06-16 20:56	-	dimming S10W10	-	-
2010-08-04 10::00	550	13	08-01 13:42	-	C3.2 N20E36	-	-	-
2010-12-20 02:00	390	9	-	12-15 12:24	-	-	unclear	-
2010-12-28 08:00	350	13	-	12-23 05:00	-	FE N25W5	-	-
2011-02-18 21:00	500	14	02-15 02:24	-	X2.2 S20W12	dimming	-	-
2011-03-30 01:00	380	13	-	03-25 14:36	C1.0 S16E31	-	-	-
2011-05-28 10:00	500	12	-	-	-	-	unclear	-
2011-06-05 02:00	550	22	06-02 08:12	-	C3.7 S18E28	dimming	-	-
2011-09-10 00:00	500	10	09-06 02:24	-	M5.3 N14W16	-	-	-
2011-09-17 18:00	430	13	-	09-14 00:00	C2.9, N23W21	dimming	-	-

Table 1. (continued)

	MC		CME		Solar Disk Activity			
Time	V (km/s)	Halo	P.Halo	Flare	Other	Unclear	None	
2011-10-25 00:00	525	24	10-22 01:25	-	-	FE N30W30	-	-
2012-01-02 20:00	400	12	-	12-29 16:24	-	-	unclear	-
2012-01-22 23:30	410	14	1-19 14:36	-	M3.2 N28E13	dimming	-	-
2012-02-15 00:00	390	9	2-10 20:00	-	B9.9 N35E30	FE	-	-
2012-03-09 00:30	700	17	03-07 00:24	-	X5.4 N17E15	dimming	-	-
2012-03-15 21:00	700	15	03-10 18:00	-	M8.4 N18W27	dimming	-	-
2012-04-23 20:00	380	16	uncertain	uncertain			few activity	
2012-05-04 02:00	310	8	uncertain	uncertain			uncertain	
2012-05-16 21:00	370	12	05-12 00:00	-	C3.2	dimming	-	-
2012-06-11 15:00	400	10	uncertain	uncertain			uncertain	
2012-06-16 23:00	500	40	06-14 14:12	-	M1.9 S17W00	dimming	-	-
2012-07-09 00:00	410	12	07-04 17:24	-	M1.8 N16W36	dimming	-	-
2012-07-15 07:00	699	27	07-12 16:48	-	X1.4 S17W08	FE		
2012-09-30 23:00	400	21	09-28 00:12	-	C3.7 N09W26	dimming FE	-	-
2012-10-08 12:00	400	16	-	10-05 02:48	B7.8 S35W26	dimming FE	-	-
2012-10-12 17:00	470	12	-	10-07 07:36	B4.5 S40W35	dimming FE	-	-
2012-11-01 00:30	360	15	10-27 16:48	-	B7.3 N25W30	dimming	-	-
2012-11-13 08:00	380	21	-	11-09 15:12	GOES gap S25E25	FE	-	-

[a]FE: filament eruption.

interplanetary medium [*Wang et al.*, 2002, 2004; *Zhang et al.*, 2003]. Based on observation data and a kinetic analysis, *Wang et al.* [2004] concluded that fast CMEs are deflected to the east and slow CMEs to the west.

The magnetic structure of coronal mass ejections (CMEs) originates at the low atmosphere of the Sun. The interplanetary coronal mass ejections (ICMEs) that exhibit the topology of helical magnetic flux ropes are referred to as magnetic clouds (MCs) [*Klein and Burlaga*, 1982; *Zhang and Burlaga*, 1988; *Bothmer and Schwenn*, 1998]. MC flux ropes with axis of low (high) inclination with respect to the ecliptic plane are called bipolar (unipolar) MCs. The poloidal field of bipolar MCs has a solar cycle dependence. A cyclic reversal of the bipolar MC poloidal field on the same time scale of the solar magnetic cycle is found during 1976 to 2009 spanning over three sunspot cycles [*Li et al.*, 2011, and references therein].

In this paper we analyze data from STEREO A (STA) and STEREO B (STB) and ACE spacecraft spanning years 2007 to 2012. We examine the MCs at each observing point and the variation of MC properties with solar activity. We track the CME sources near the Sun for those MCs that encountered the Earth. In the first
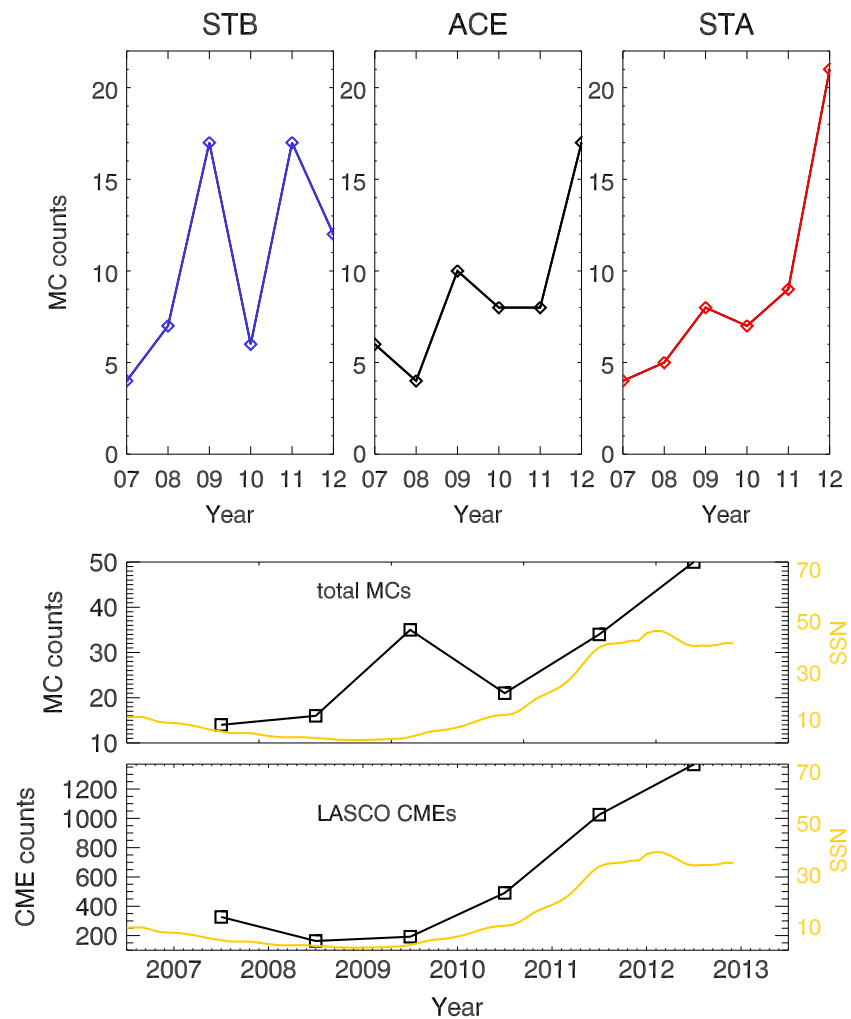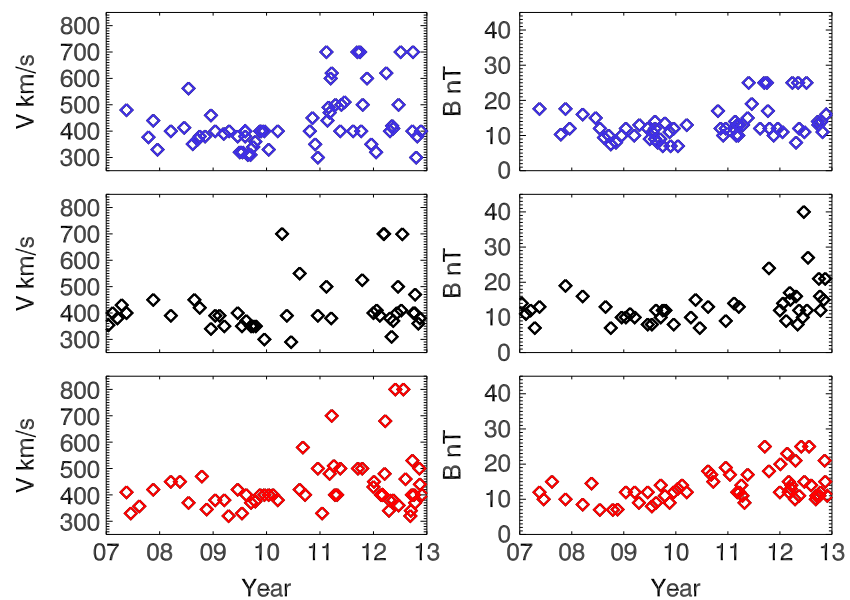
Figure 1. (top) (left) MC annual counts at STEREO B against year, (center) MC counts at ACE against year, and (right) MC annual counts at STEREO A against year. (middle) Total MC annual counts at all three points for each year (black) and smoothed monthly sunspot number (yellow). (bottom) Annual counts of LASCO CMEs with angular width greater than 30° (black) and smoothed monthly sunspot number (yellow).

couple of years of the STEREO mission, researchers have noticed that STEREO B spacecraft received many more MCs than the other two points, and it has been puzzling in our research community. This is one of our motivations for this study. The goal of this study is to investigate MC properties' solar cycle variation and how much fluctuation MC counts can be at any point at 1 AU near the ecliptic plane, through comparison between results from the three spacecraft. We also investigate the MC and CME correspondence and MC's solar sources through multispacecraft data.

2. MC Encounters at Each Point: L1, STEREO A and B

We use STEREO A and B 10 min IMPACT and PLASTIC merged level 2 data that are archived at UCLA. Through examining the IMF three components and the solar wind plasma parameters of proton temperature, density and bulk speed, and the plasma beta, we select MC intervals. Using the same parameters of 1 min data by ACE spacecraft at L1 point, we select MCs that encountered the Earth. To identify MCs, we require (1) an enhanced magnetic field magnitude greater than ≈7nT, (2) a low-variance magnetic field with a coherent rotation of the field vector over a time interval on the order of a day, and (3) a lower than average proton temperature. The same criteria are used for the data from all spacecraft. The selection process is simply by visual inspection, in the same manner with previous studies [*Mulligan et al.*, 1998; *Li et al.*, 2011], based on which we extend the MC polarity study. MC annual counts are recorded for the past 7 years from 2007 to

Figure 2. MC speed and the peak MC magnetic field for each event against time at (top) STEREO B, (middle) ACE, and (bottom) STEREO A.

2012. We have 47 MCs at L1 point from ACE, which are listed in Table 1 along with their source information, 54 MCs at STA and 57 at STB, which are listed in two separate tables as attachments of the paper. In Figure 1 (top), we plot the MC annual counts at STEREO B against year in blue curve at the left, the MC annual counts at ACE against year in black curve in the center, and the MC annual counts at STEREO A against year in red curve at the right. MC encounters at each observing point were different in both counts and temporal variation trend. It shows the relative unpredictability of MC encounters at any single observing point. The period of 2007 to 2012 begins at the late declining phase of solar cycle 23, through the solar minimum, and ends around the solar activity maximum of solar cycle 24 as shown by the smoothed monthly sunspot numbers (yellow curves) in Figures 1 (middle) and 1 (bottom). The black curve in Figure 1 (middle) gives the total MC annual counts at all three points for each year, and the black curve in Figure 1 (bottom) is the annual counts of Large Angle and Spectrometric Coronagraph (LASCO) CMEs with angular width greater than 30°. The CME annual counts range from 200 to 800 and the variations follow the solar activity level. The MC annual counts range from 4 to 21 at any single observing point, and the annual counts of the sum of the three observing points range from 14 to 50. There are in total 54 MCs at STA, 57 MCs at STB, and 47 MCs at L1 point, which add to 158 MCs (including a few MCs that are different crossings of the same CMEs in year 2007) observed at 1 AU ecliptic plane during the 7 years since the operation of STEREO mission. It is apparent that only a small fraction of CMEs result in MCs seen at 1 AU in the ecliptic plane.

In Figure 2, we show the MC peak speed and the MC peak magnetic field of each event against time at STEREO B (top), ACE (middle), and STEREO A (bottom). The MC speed ranges from 300 km/s to 800 km/s (see Table 1 for the actual values of the speed). The MC speed shows a solar activity dependence, and MCs at the solar minimum 2009 have the lowest speed. The total magnetic field strength ranges from 7 to 40 nT and also shows a solar cycle dependence with the MC at solar minimum having the weakest field. In Figure 3, we show the distribution of the MC speed for the three observing points: at STA the MC occurrence peaks at around 370 km/s, at STB around 390 km/s, and at L1 the MC number peaks at 400 km/s. The magnetic field strength distribution (right) is similar at all three points with the peak number at around 11 nT. The maximum of the MC peak magnetic strength in this group is about 40 nT, but only one MC at this value, and magnetic field strength of the rest of the MCs is all below 30 nT.

3. Solar Cycle Dependence of MCs Magnetic Field Structure

Li et al. [2011] reported the solar cycle dependence of the MC field polarity combining data from 1976 to 2009. When a bipolar MC traverses an observer and the north-south component of the MC show north
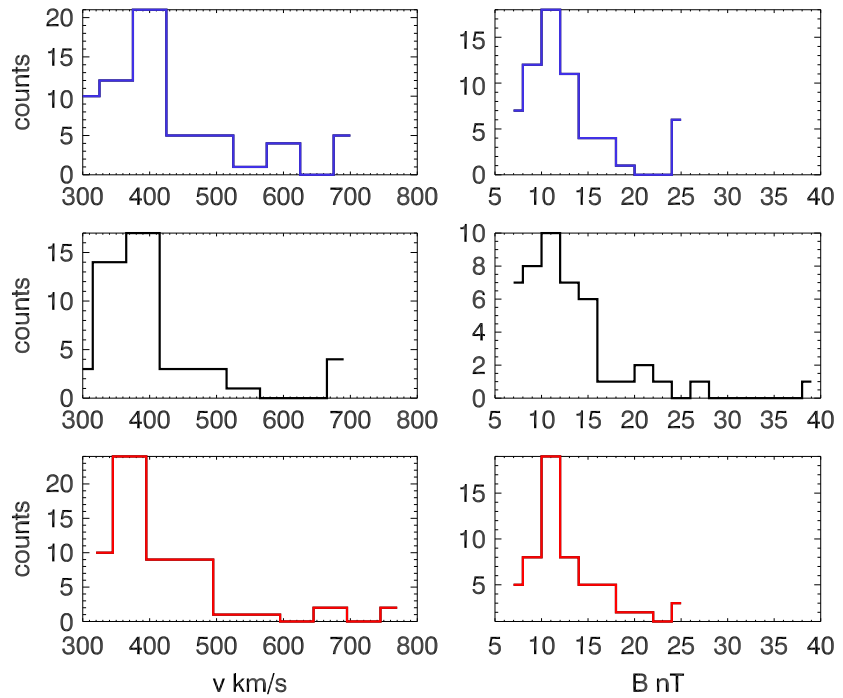
Figure 3. (left) The distribution of the MC speed is similar at the three points with the peak number at around 370, 390, and 400 km/s slightly below the average solar wind speed. (right) The magnetic field strength distribution is also similar at all three points with the peak number at around 11 nT.
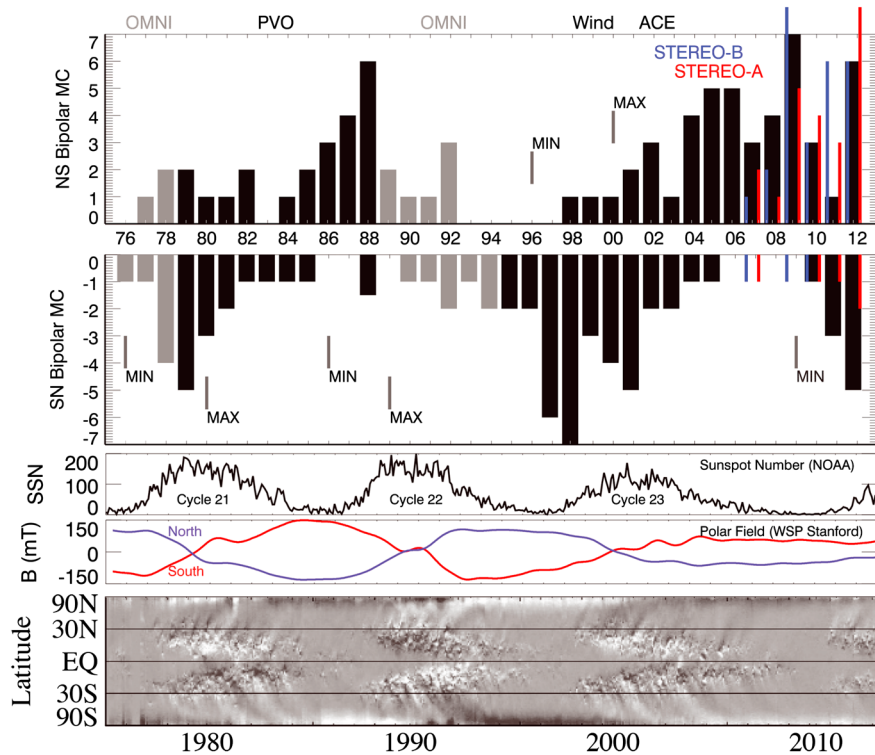
Figure 4. (top) Bipolar MC field solar cycle dependence. (middle) Reference parameters of solar cycle: sunspot numbers and solar polar magnetic field. (bottom) Solar magnetic butterfly diagram.
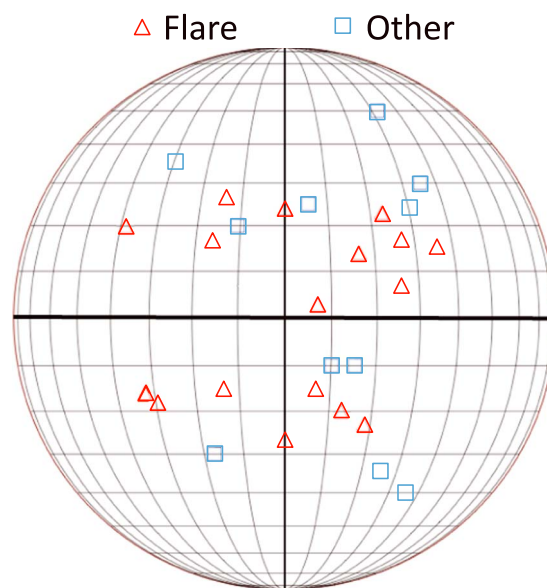
Table 2. Summary: L1 Magnetic Clouds and Origins in 2007–2012

		CME			Solar Disk Activity		
Year	MC	Halo	P.Halo	None	Flare	Other	Unclear	None
2007	3	0	1	2	1	0	1	1
2008	4	0	2	2	0	3	1	0
2009	8	0	1	7	0	1	2	5
2010	8	3	4	1	4	3	0	2
2011	7	4	2	1	6	1	0	1
2012	17	10	4	3	10	6	1	2
total	47	17	14	16	21	14	5	11

(south) first then south (North), it is an NS (SN) type MC. They showed that, in bipolar MCs, the north-south component (Bz) reverses with the same periodicity as the solar magnetic field. This finding is interesting not only because it shows the connection between the MC magnetic field structure and the solar magnetic field but also because the Bz field has important space weather implications. In the current study, we extended the previous results to 2012 using ACE data. In addition, we analyzed MCs at STEREO A and B. The extended and combined results are shown in Figure 4 (top). Previous result and L1 result are indicated using black and grey bars. Results from STEREO A are indicated as red bars and STEREO B as blue bars. In the previous two solar cycles, the MC field polarity has the same orientation on the rising phase of the cycle between the solar minimum and solar maximum, and the polarity reversed on the declining phase between the solar maximum and the next minimum. The last solar minimum occurred in 2008 December, and in 2012 the Sun is on its way to reach the maximum of cycle 24. Our results from L1 (black bars) and STEREO (red and blue bars) show that, up to year 2010, the MC field polarity follows the previous trend and MCs are mostly NS type with a few exceptions. If the MC field solar cycle trend persists, we expect the MC field to remain NS through the solar maximum. Our results show that while STEREO MCs stay mostly NS type in 2011 and 2012, L1 MC field has significant fluctuations between the NS and SN types. It is difficult to say weather the MC field polarity cyclic trend breaks down at this point. We need to wait for a few more years until the solar maximum passes. Figure 4 (bottom) gives the reference parameters of the solar magnetic cycle, including the sunspot numbers, solar polar magnetic field, and the magnetic butterfly diagram.

Figure 5. MC source locations on the solar disk. Red triangles indicate flares, and blue squares indicate other activity (filament eruptions, dimming, and such).
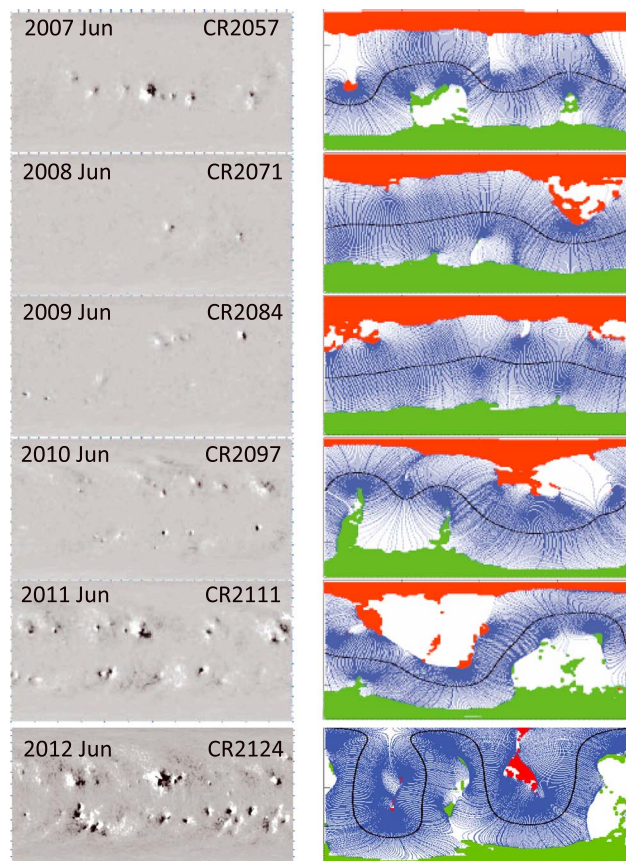
4. The Solar Sources of L1 MCs

We have identified 47 MCs that encountered the Earth. For these events, we further identify their parent CMEs and source activity near the solar surface. The results are listed in Table 1. For an MC event at L1 point (ACE), we first search the LASCO CME catalog for halo or partial halo CMEs during the 5 days prior to the MC arrival. For events after about 2008 when STEREO twin spacecraft had significant separation, we also use STEREO coronagraph and harvest indices (HI) images for better certainty of the correspondence. During solar minimum years, most MCs had no preceding halo or partial halo CMEs in LASCO images. For half of these MCs, STEREO narrow or faint limb CMEs are found near the ecliptic plane toward the Earth and are taken as possible parent CMEs of the MCs; the other half of the MCs had no reasonable parent CMEs using STEREO/SECCHI images. During the more active years, STEREO coronagraph and HI images are extremely

Table 3. MC and LASCO Halo CMEs

Year	MC	Source Halo CME	Total Halo CME
2007	3	0	3
2008	4	0	1
2009	8	0	1
2010	8	3	11
2011	7	4	41
2012	17	10	84
total	47	17	141

useful for distinguishing the Earth-impacting CMEs from multiple events. Our experience is that it is either hard to find any parent CME at the solar minimum or too many possible parent CMEs as soon as the Sun begins to be active. Once the parent CMEs are identified, we further identify the associated activity in the low corona. The activity includes solar flares, filament eruptions, and EUV dimming. In Table 1, we give the MC arrival time at L1 point (ACE), the peak speed and the peak value of the magnetic field strength of the MCs. We also give the time of the halo CME or partial halo CME prior to an MC and the type of associated solar activity. When there is some activity on the solar disk at the time of a CME, but it is unclear which activity is the source for the particular CME, we put "unclear," and when there is no activity at all on the solar disk at the time of a CME, we put "none."

Table 2 summarizes, for each year, the number of MCs at L1 and their corresponding CMEs and solar activity. In solar minimum year 2009, seven out of eight MCs had no preceding halo or partial halo CMEs in the LASCO view. Five out of the eight cases had no activity on the visible solar disk. In the most active year 2012, 10 MCs had preceding LASCO halo CME, four had preceding partial halo CMEs, and three had no preceding halo or partial halo CME. Ten out of the 17 cases had companion flares. Combining the 5 years, 17 out of 47 MCs had preceding LASCO halo CMEs, 14 had preceding partial halo CMEs, and 16 had neither halo nor partial halo CMEs within the 5 days prior to the MCs. Twenty-one out of 47 events had flares, and 14 had other activity. Five had unclear sources, and 11 had no activity at all on the solar disk. In Figure 5, we mark the MC source locations on the solar disk. Red triangles indicate flares, and blue squares indicate other activity (filament eruptions, dimming, and such). The source locations of these Earth-impacting CMEs are within about 40° of solar latitude and longitude with one outlier.

Table 3 summarizes the annual counts of MCs, the number of halo CMEs that are MC sources, and the annual counts of all halo CMEs. In year 2007, there are three MCs and three halo CMEs, but they do not correspond to each other. In 2012, there are 17 MCs and 84 halo CMEs, with 10 of them corresponding to each other. Overall, there are 47 MCs and 141 halo CMEs during the 6 years from 2007 to 2012, with only 17 corresponding to each other. This result is somewhat surprising, because it disagrees with previous studies and our common sense, see section 1 and the next section for discussions.

5. Summary, Discussions, and Conclusions

We have made use of solar wind IMF in situ data and solar coronal imaging data obtained by STEREO twin spacecraft, ACE and SOHO spacecraft at three observing points near

Figure 6. (left) Synoptic map of GONG. (right) PFSS model coronal holes, Helmet streamer, and source surface neutral line.

1 AU around the ecliptic plane during the 6 years from 2007 to 2012. We found that at the three independent observing points, the number of MCs seen at each point varies significantly. The temporal trend of annual MC counts in the 6 years at each observer also differs from one another, and did not always follow the solar activity trend, unlike the number of CMEs observed by coronagraph images. Our result shows that the chance of receiving MCs at any single point in the heliosphere is often unpredictable, making the space weather forecasting a difficult job. The speed and magnetic strength carried by the MCs do vary with the solar activity cycle, i.e., the MC speed is higher at solar maximum and lower at minimum, and the MC internal magnetic field is stronger at solar maximum and weaker at solar minimum. This study is not intended to be an inclusive statistic study of ICMEs. We only study MCs, which is one of the most identifiable type of ICME, and our focus is the comparison of MC properties among the three observing points to gain knowledge of their fluctuations in space. We refer ICME and/or MCs statistics to other studies in the literature, e.g., *Huttunen et al.* [2005], *Wu and Lepping* [2011], and *Lepping et al.* [2011] in addition to a few others cited earlier.

We note that all three spacecraft had relatively more MC encounters in the solar minimum year 2009, although the number of CMEs in coronagraph images is minimum in 2009. We can perhaps attribute this fact to the coronal magnetic field dipolar configuration at the solar minimum that channels more CMEs to the ecliptic plane, as argued previously by *Cremades et al.* [2006]. Shown in Figure 6 (left) are the synoptic maps and (right) PFSS model coronal helmet streamer field lines (blue lines), source surface neutral line (black line), and coronal hole area (red and green). We selected one synoptic map per year of the 6 years we studied as shown in Figure 6. The coronal field was the most dipolar in 2009 (the third row), consistent with what is expected.

Our new extended MC field polarity result presents a largely consistent picture with our previous report in *Li et al.* [2011], except for some fluctuations in L1 MC polarity. We think that the excursion from the cyclic trend seen in L1 MC polarity in 2011–2012 is a temporary fluctuation, perhaps related to the more multipolar coronal field geometry of the current weak cycle [e.g., *Petrie*, 2013]. Fluctuations as such should also be natural in small number statistics. We expect the MC polarity cycle to persist, but it cannot be completely conclusive at this point before cycle 24 ends in a few years.

We have identified the parent CMEs of the Earth-impacting MCs, using SOHO/LASCO and STEREO/SECCHI images taken from different viewing points to minimize ambiguity. For the total 47 MCs at the L1 point, 17 were from LASCO halo CMEs, 14 were from LASCO partial halo CMEs, and 16 had neither halo nor partial halo during the 5 days before. We find that halo CMEs are statistically poor indicators for MCs at the observer. In other words, halo CMEs are generally not good predictors for MCs at the point of halo observation. There were a total of 141 LASCO full halo CMEs during the 6 years, only 17 of them encountered Earth as MCs. Assuming half of them were backsided, it means about 70 frontside full halo CMEs versus 17 MCs at Earth. According to our results in this study, a halo CME is neither sufficient nor necessary for an observer to receive an MC.

Some believe that an MC is the flux rope core of an ICME, i.e., a part contained in a larger structure. If one selects ICMEs instead of MCs, more cases may be found. The ratio between MCs and ICMEs has been reported previously, and it is solar cycle dependent [*Cane and Richardson*, 2003; *Richardson and Cane*, 2010; *Li et al.*, 2011]. The MC and ICME ratio varies between 1:1 to 1:3 from solar minimum to solar maximum. The ratio of the total number of events in solar cycle 23 was slightly under 1:2 between MCs and ICMEs [*Li et al.*, 2011]. Applying this ratio here, it gives about 70 full halo CMEs versus roughly 30 ICMEs. Slightly less than half of the halo CMEs encounter the Earth as ICMEs, which makes halo CMEs a somewhat better predictor for ICMEs than MCs, but still only modestly successful.

As pointed out in the previous section, our results that halo CMEs are poor indicators of MCs appear to be in disagreement with the common perception and some previous reports. *Webb et al.* [2000] analyzed 14 halo CMEs from the post solar minimum years 1996 and 1997 and seven are frontside events. Six of the seven frontside halo CMEs had MCs and moderate magnetic storms at Earth 3 to 5 days later. *Gopalswamy et al.* [2007] found that 71% halo CMEs during 1996 to 2005 are geoeffective using *Dst* index without identifying MCs. These studies gave different ratio than our result between LASCO halo CMEs and their arrival at Earth. However, *Webb et al.* [2000] studied about a dozen halo CMEs all from near solar minimum years, and *Gopalswamy et al.* [2007] compared halo CMEs directly with *Dst* index. We believe our result about halo CME and MC correspondence is more comprehensive and credible, given the fact that we have identified MC and

CME pairs for a larger number of events during half of a solar cycle with the assistance of CME images from three viewing angles.

We further identified the activity on the solar disk associated with our group of events. We found that 21 of the 47 MCs had flare activity, 14 had other activity on the solar disk (including prominence eruption, coronal dimming, post CME arcades, and such), five had unclear sources, and 11 events had no activity at all on the solar disk, i.e., stealth CMEs [*Robbrecht et al.*, 2009; *Lynch et al.*, 2010]. The solar activity associated with this group of CMEs that encountered Earth did not seem to favor one type or another of activity but was spread over all types of activity known to be related to CMEs in general. The locations of this group of CMEs had sources on the Sun within 40° from the center of the solar disk with the exception of one event. The number of CMEs having west hemispheric origins was somewhat larger than the number with east hemispheric origins at the ratio 17:10.

Whether or not a halo CME will impact the Earth can be influenced by a number of factors. We believe the factors should include CME initial direction, CME interaction with the surrounding corona, CME interaction with the solar wind during its propagation in interplanetary space, and such. Detailed studies are needed about these issues in order to fully understand the motion of CMEs and to improve our space weather forecasting capability.

References

Bothmer, V., and R. Schwenn (1998), The structure and origin of magnetic clouds in the solar wind, *Ann. Geophys.*, 16, 1–24.

Cane, H. V., I. G. Richardson, and O. C. St. Cyr (2000), Coronal mass ejections, interplanetary ejecta and geomagnetic storms, *Geophys. Res. Lett.*, 27, 3591–3594.

Cane, H. V., and I. G. Richardson (2003), Interplanetary coronal mass ejections in the near-Earth solar wind during 1996–2002, *J. Geophys. Res.*, 108(A4), 1156, doi:10.1029/2002JA009817.

Cremades, H., V. Bothmer, and D. Tripathi (2006), Properties of structured coronal mass ejections in solar cycle 23, *Adv. Space Res.*, 38, 461–465.

Gopalswamy, N., S. Yashiro, and S. Akiyama (2007), Geoeffectiveness of halo coronal mass ejections, *J. Geophys. Res.*, 112, A06112, doi:10.1029/2006JA012149.

Gopalswamy, N., S. Akiyama, S. Yashiro, G. Michalek, and R. P. Lepping (2008), Solar sources and geospace consequences of interplanetary magnetic clouds observed during solar cycle 23, *J. Atmos. Sol. Terr. Phys.*, 70, 245–253.

Huttunen, K. E. J., R. Schwenn, V. Bothmer, and H. E. J. Koskinen (2005), Properties and geoeffectiveness of magnetic clouds in the rising, maximum and early declining phases of solar cycle 23, *Ann. Geophys.*, 23, 625–641.

Kilpua, E. K. J., J. Pomoell, A. Vourlidas, R. Vainio, J. Luhmann, Y. Li, P. Schroeder, A. B. Galvin, and K. Simunac (2009), STEREO observations of interplanetary coronal mass ejections and prominence deflection during solar minimum period, *Ann. Geophys.*, 27, 4491–4503.

Klein, L. W., and L. F. Burlaga (1982), Interplanetary magnetic clouds at 1 AU, *J. Geophys. Res.*, 87(A2), 613–624, doi:10.1029/JA087iA02p00613.

Lepping, R. P., C.-C. Wu, D. B. Berdichevsky, and A. Szabo (2011), Magnetic clouds at/near the 2007–2009 solar minimum: Frequency of occurrence and some unusual properties, *Sol. Phys.*, 274, 345–360.

Li, Y., J. G. Luhmann, B. J. Lynch, and E. K. J. Kilpua (2011), Cyclic reversal of magnetic cloud poloidal field, *Sol. Phys.*, 270, 331–346.

Lynch, B. J., Y. Li, A. F. R. Thernisien, E. Robbrecht, G. H. Fisher, J. G. Luhmann, and A. Vourlidas (2010), Sun to 1 AU propagation and evolution of a slow streamer-blowout coronal mass ejection, *J. Geophys. Res.*, 115, A07106, doi:10.1029/2009JA015099.

Mulligan, T., C. T. Russell, and J. G. Luhmann (1998), Solar cycle evolution of the structure of magnetic clouds in the inner heliosphere, *J. Geophys. Res.*, 25, 2959–2962.

Petrie, G. J. D. (2013), Solar magnetic activity cycles, coronal potential field models and eruption rates, *Astrophys. J.*, 768, 18.

Richardson, I. G., and H. V. Cane (2010), Near-Earth interplanetary coronal mass ejections during solar cycle 23 (1996–2009): Catalog and summary of properties, *Sol. Phys.*, 264, 189–237.

Robbrecht, E., S. Patsourakos, and A. Vourlidas (2009), No trace left behind: STEREO observation of a coronal mass ejection without low coronal signatures, *Astrophys. J.*, 701, 283.

Wang, Y. M., P. Z. Ye, S. Wang, G. P. Zhou, and J. X. Wang (2002), A statistical study on the geoeffectiveness of Earth-directed coronal mass ejections from March 1997 to December 2000, *J. Geophys. Res.*, 107(A11), 1340, doi:10.1029/2002JA009244.

Wang, Y., C. Shen, S. Wang, and P. Ye (2004), Deflection of coronal mass ejection in the interplanetary medium, *Sol. Phys.*, 222, 329–343.

Webb, D. F., E. W. Cliver, N. U. Crooker, O. C. St. Cyr, and B. J. Thompson (2000), Relationship of halo coronal mass ejections, magnetic clouds, and magnetic storms, *J. Geophys. Res.*, 105, 7491–7508.

Wu, C.-C., and R. P. Lepping (2011), Statistical comparison of magnetic clouds with interplanetary coronal mass ejections for solar cycle 23, *Sol. Phys.*, 269, 141–153.

Zhang, G., and L. F. Burlaga (1988), Magnetic clouds, geomagnetic disturbances, and cosmic ray decreases, *J. Geophys. Res.*, 93, 2511–2518.

Zhang, J., K. P. Dere, R. A. Howard, and V. Bothmer (2003), Identification of solar sources of major geomagnetic storms between 1996 and 2000, *Astrophys. J.*, 582, 520–533.